Video Article

SNARE-mediated Fusion of Single Proteoliposomes with Tethered Supported Bilayers in a Microfluidic Flow Cell Monitored by Polarized TIRF Microscopy

Joerg Nikolaus[1,2], Erdem Karatekin[1,2,3,4]

[1]Department of Cellular and Molecular Physiology, Yale University School of Medicine

[2]Nanobiology Institute, Yale University

[3]Department of Molecular Biophysics and Biochemistry, Yale University

[4]Laboratoire de Neurophotonique, Université Paris Descartes, Faculté des Sciences Fondamentales et Biomédicales, Centre National de la Recherche Scientifique (CNRS)

Correspondence to: Erdem Karatekin at erdem.karatekin@yale.edu

URL: https://www.jove.com/video/54349
DOI: doi:10.3791/54349

Keywords: Neuroscience, Issue 114, Membrane fusion, SNARE proteins, lipid bilayer, proteoliposomes, supported bilayer, single vesicle fusion, fusion pore, exocytosis, single-molecule fluorescence, microfluidics, TIRFM, biophysics

Date Published: 8/24/2016

Citation: Nikolaus, J., Karatekin, E. SNARE-mediated Fusion of Single Proteoliposomes with Tethered Supported Bilayers in a Microfluidic Flow Cell Monitored by Polarized TIRF Microscopy. *J. Vis. Exp.* (114), e54349, doi:10.3791/54349 (2016).

Abstract

In the ubiquitous process of membrane fusion the opening of a fusion pore establishes the first connection between two formerly separate compartments. During neurotransmitter or hormone release via exocytosis, the fusion pore can transiently open and close repeatedly, regulating cargo release kinetics. Pore dynamics also determine the mode of vesicle recycling; irreversible resealing results in transient, "kiss-and-run" fusion, whereas dilation leads to full fusion. To better understand what factors govern pore dynamics, we developed an assay to monitor membrane fusion using polarized total internal reflection fluorescence (TIRF) microscopy with single molecule sensitivity and ~15 msec time resolution in a biochemically well-defined *in vitro* system. Fusion of fluorescently labeled small unilamellar vesicles containing v-SNARE proteins (v-SUVs) with a planar bilayer bearing t-SNAREs, supported on a soft polymer cushion (t-SBL, t-supported bilayer), is monitored. The assay uses microfluidic flow channels that ensure minimal sample consumption while supplying a constant density of SUVs. Exploiting the rapid signal enhancement upon transfer of lipid labels from the SUV to the SBL during fusion, kinetics of lipid dye transfer is monitored. The sensitivity of TIRF microscopy allows tracking single fluorescent lipid labels, from which lipid diffusivity and SUV size can be deduced for every fusion event. Lipid dye release times can be much longer than expected for unimpeded passage through permanently open pores. Using a model that assumes retardation of lipid release is due to pore flickering, a pore "openness", the fraction of time the pore remains open during fusion, can be estimated. A soluble marker can be encapsulated in the SUVs for simultaneous monitoring of lipid and soluble cargo release. Such measurements indicate some pores may reseal after losing a fraction of the soluble cargo.

Video Link

The video component of this article can be found at https://www.jove.com/video/54349/

Introduction

Membrane fusion is a universal biological process required for intracellular trafficking of lipids and proteins, secretion, fertilization, development, and enveloped virus entry into host organisms[1-3]. For most intracellular fusion reactions including release of hormones and neurotransmitters via exocytosis, the energy to fuse two lipid bilayers is provided by formation of a four-helix bundle between cognate *soluble N-ethylmaleimide-sensitive factor attachment protein receptor* (SNARE) proteins, anchored in the vesicle (v-SNARE) and the target membrane (t-SNARE)[4], respectively. Synaptic vesicle exocytosis is the most tightly regulated fusion reaction and occurs within a millisecond after the arrival of an action potential[1,4,5]. The fusion pore, the initial connection between the two fusing compartments, can flicker open and closed multiple times before resealing or expanding irreversibly[5-7]. The former results in transient, "kiss & run" fusion, while the latter leads to full fusion. Factors governing the balance between these two modes of fusion and mechanisms regulating pore flickering are not well understood[5,8].

SNARE proteins are required for exocytosis; synaptic vesicle fusion is abolished upon cleavage of SNAREs by neurotoxins[9]. Bulk fusion experiments using small unilamellar vesicles (SUVs) showed that SNAREs are not only required, but also sufficient to drive membrane fusion[10]. In this bulk assay, SUVs reconstituted with v-SNAREs (v-SUV) were doped with fluorescent phospholipids (*N*-(7-nitro-2-1,3-benzoxadiazol-4-yl)-phosphoethanolamine (NBD-PE) and (*N*-(lissamine rhodamine B sulfonyl)-phosphoethanolamine (LR-PE) and mixed with unlabeled vesicles containing t-SNAREs (t-SUV). Initially the fluorescence of NBD-PE in v-SUVs is quenched by Förster resonance energy transfer (FRET) to LR-PE. As labeled v-SUVs fuse with unlabeled t-SUVs, the fluorophore surface density in the now combined membrane is reduced and the resulting increase in NBD-PE fluorescence reports the extent of lipid mixing[10]. As the bulk assay is easy to set up and analyze, it has been widely used to study mechanisms of SNARE-mediated fusion[10-14]. However, it has several limitations, such as low sensitivity and poor time resolution. Most

importantly, as an ensemble measurement, it averages results over all events making discrimination between docking and fusion, as well as detection of hemifusion intermediates difficult.

Over the past decade several groups, including ours, have developed new assays to monitor fusion events at the single vesicle level[15-27]. Ha and colleagues used v-SUVs tethered onto a surface and monitored their fusion with free t-SUVs[18,19]. Lipid mixing was monitored using FRET between a pair of lipid-bound fluorophores embedded in the v- and t-SUVs, respectively, using total internal reflection fluorescence (TIRF) microscopy[18]. Later, Brunger's laboratory used a single lipid-label species together with a contents marker for simultaneous detection of lipid and contents mixing[20,28]. Both the lipid and the contents markers were included at high, self-quenching concentrations; fusion with unlabeled SUVs resulted in fluorescence dequenching[20,28].

Others have fused v-SUVs to planar bilayers reconstituted with t-SNAREs[15-17,21-27,29]. The planar geometry of the target (t-SNARE containing) bilayer better mimics the physiological fusion process of small, highly curved vesicles with a flat plasma membrane. The Steinem group employed pore-spanning membranes reconstituted with t-SNAREs, suspended over a porous silicon nitride substrate and detected fusion with individual v-SUVs using confocal laser scanning microscopy[23]. Others fused v-SUVs to planar bilayers reconstituted with t-SNAREs, supported on a glass substrate[15-17,21,22,24-27,29]. The great advantage of using supported bilayers (SBLs) is that TIRF microscopy can be used to detect docking and fusion events with excellent signal-to-noise ratio and without interference from free v-SUVs, although using microfluidics also provides single-event resolution using standard far-field epifluorescence microscopy[24].

A major concern is whether and how substrate-bilayer interactions affect supported bilayer quality and the fusion process. Early work made use of planar SBLs that were directly supported on a glass or quartz substrate[15-17]. These SBLs were made by adsorption, bursting, spreading and fusion of t-SUV membranes on the substrate. It was soon realized, however, that omitting a key t-SNARE component, SNAP25, from SBLs prepared in this manner resulted in v-SUV docking and fusion kinetics indistinguishable from those obtained using the complete t-SNAREs[17]. Because SNAP25 is absolutely required for fusion *in vivo*[30,31], the physiological relevance of these early attempts was put into question. Tamm's group overcame this challenge by using better controlled supported bilayer formation[21]. It used Langmuir-Blodgett deposition for the protein-free first leaflet of the SBL, followed by fusion of that monolayer with t-SUVs[21]. This resulted in SNAP25-dependent fusion.

To avoid potential artefacts associated with a bilayer directly supported on a glass substrate without need to use Langmuir-Blodgett methods, Karatekin *et al.* introduced a soft, hydrated poly(ethylene glycol) (PEG) cushion between the bilayer and the substrate[24]. This modification also resulted in SNAP25-dependent fusion[24]. Bilayers cushioned on a soft polymer layer had been known to better preserve transmembrane protein mobility and function[32], and had been used in fusion studies with viruses[33]. In addition, PEGylated bilayers seem to retain some ability to self-heal and are very robust[34,35]. First, a fraction of commercially available, lipid-linked PEG chains are included in the t-SUV membrane. When these t-SUVs burst and form a planar bilayer on a glass substrate, a PEG brush covers both leaflets of the planar bilayer. Because planar bilayer formation is driven by adhesion of the PEG chains surrounding t-SUVs onto the hydrophilic glass surface, liposome bursting and planar bilayer formation are relatively insensitive to the lipid composition used. However, when large amounts of cholesterol are included, increasing the cohesive properties of the SUVs, the SUVs may not burst spontaneously. If this is the case, osmotic shock or divalent ions can be employed to help planar bilayer formation[25].

As mentioned above, in this approach a PEG brush covers both sides of the planar, supported bilayer. The brush facing the microfluidic flow channel helps to prevent nonspecific adhesion of incoming v-SUVs which are also usually covered with a PEG layer. Formation of v- and t-SNARE complexes starts from the membrane-distal N-termini and proceeds in stages toward the membrane-proximal domains[36]. For the v-SUVs to interact with the t-SBL, the v- and t-SNARE N-termini need to protrude above the PEG brushes, which seems to be the case under the conditions of the assay. Brush height can be adapted to study proteins other than SNAREs by varying the density of PEGylated lipids and the PEG chain length[37,38]. Another benefit of the PEG brushes covering the proximal surfaces of the fusing bilayers is that they mimic the crowded environment of biological membranes which are packed with 30,000-40,000 integral membrane proteins per square micron[39]. Just like the PEG chains in this assay, the repulsive protein layer covering biological membranes needs to be pushed aside to allow for contact between the two phospholipid bilayers for fusion to occur.

Microfluidic flow channels are used in this assay, as they offer unique advantages. First, microfluidic flow enables more uniform deposition of t-SUVs to spread and fuse to form the t-SBL. Second, the small channel volume (< 1 µl) minimizes sample consumption. Third, the small volumes required allow the entire experiment to be conducted under constant flow. Flow removes weakly, presumably non-specifically, adhered v-SUVs from the SBL[16]. It also maintains a constant density of v-SUVs above the t-SBL, simplifying kinetic analysis[17]. Finally, docked vesicles are easily distinguished from free ones carried by the flow[25]. Fourth, several microfluidic channels can be used on the same coverslip, each probing a different condition. This allows comparison of conditions during the same experimental run. A similar approach has been used by the van Oijen group to study fusion between influenza virus and cushioned SBLs[33].

In TIRF microscopy, the exponential decay of the evanescent field (with a decay constant ~100 nm) confines fluorescence excitation to those molecules that are in very close proximity of the glass-buffer interface. This minimizes contribution of fluorescent molecules that are further away, increases the signal-to-noise ratio, and allows single molecule sensitivity with frame exposure times of 10-40 msec. The evanescent field also leads to a signal increase upon fusion: as the labeled lipids transfer from the SUV into the SBL, they find themselves, on average, in a stronger excitation field. This increase in fluorescence is stronger for larger liposomes.

If polarized light is used to generate the evanescent field, additional effects contribute to changes in fluorescence upon transfer of labels from the SUV into the SBL. Some lipid dyes have a transition dipole oriented with a preferred mean angle with respect to the bilayer in which they are embedded. This creates a difference in the amount of fluorescence emitted by the fluorophores when they are in the SUV *versus* the SBL, since the polarized beam will excite dyes in the two membranes differently. For the former, the excitation beam will interact with transition dipoles oriented around the spherical SUV, whereas for the latter, dipole orientations will be confined by the flat SBL geometry. For example, when s-polarized incident light (polarized normal to the plane of incidence) is used, excitation is more efficient when the dye is in the SBL than in the SUV for a lipid dye transition dipole oriented parallel to the membrane[29,40] (such as that of DiI or DiD[41-43]). A SUV doped with such a fluorophore appears dim when it docks onto the SBL (**Figure 7**, Representative Results). As a fusion pore opens and connects the SUV and SBL membranes, fluorescent probes diffuse into the SBL and become more likely to be excited by the s-polarized evanescent field[25,27,29]. Consequently, the fluorescence signal integrated around the fusion site increases sharply during dye transfer from the SUV into the SBL[27]

(**Figure 3** and **Figure 7**). An additional factor that contributes to signal changes that accompany fusion is dequenching of fluorescent labels as they are diluted when transferred into the SBL. The contribution of dequenching is usually minor compared to evanescent field decay and polarization effects in the assay described here, because only a small fraction ($\lesssim 1\%$) of the lipids are labeled.

The signal increase upon fusion can be exploited to deduce fusion pore properties by comparing the time, τ_{ves} , required for a lipid to escape through a pore that is freely permeable to lipids to the actual release time, $\tau_{release}$. If the two time scales are comparable, it would be concluded that the pore presents little resistance to lipid flow. However, if the actual release time is significantly longer than the time for diffusion-limited release, this would indicate a process, such as pore flickering, retarding lipid release. The diffusion-limited release time, τ_{ves}, depends on the size of the fusing liposome and lipid-diffusivity; its estimation requires these two parameters to be quantified. The single molecule sensitivity of the assay allows lipid diffusivity to be measured by tracking several single lipid fluorophores after their release into the SBL for every fusion event[26]. The size of every fusing vesicle can be estimated[27] by combining (i) the intensity of a single lipid dye, (ii) the change in the total fluorescence around a docking site after all fluorophores are transferred into the SBL upon fusion, (iii) the known labeling density of SUV lipids, and (iv) the area per lipid. For many fusion events, the actual lipid release times were found to be much slower than expected by diffusion-controlled release[27], as was noted previously assuming uniform SUV size[44]. Assuming retardation of lipid release is due to pore flickering, a quantitative model allows estimation of "pore openness", the fraction of time the pore remains open during fusion[27].

Whenever practical, it is important to test fusion mechanisms using both lipid and soluble contents labels. For example, lipid release could be retarded by processes other than pore flickering, such as restriction of lipid diffusion by the SNARE proteins that surround the pore. If this were the case, then release of contents would precede release of lipid labels, provided the pore is large enough to allow passage of soluble probes. A more fundamental flaw in the approach could be in the assumption that the transfer of labeled lipids to the SBL occurs through a narrow fusion pore connecting the SBL to a vesicle that has largely retained its pre-fusion shape. Lipid transfer into the SBL could also result from rapid dilation of the fusion pore with a concomitant, extremely rapid collapse of the SUV into the SBL membrane, as previously suggested based on lipid release data alone[29]. Monitoring both lipid and contents release simultaneously, it was found that many pores reseal after releasing all their lipid labels, but retained some of their soluble cargo[27]. This indicates that at least some liposomes do not collapse into the SBL after fusion, and that the lipid dye transfer into the SBL occurs through a fusion pore. In addition, lipid and contents release occurred simultaneously[27], making it unlikely that retardation of lipid release was due to hindrance of lipid diffusion by the SNARE proteins surrounding the pore[45].

A SUV-SBL fusion protocol that did not monitor soluble contents release was previously published by Karatekin and Rothman[25]. Here, more recent developments are included, namely simultaneous monitoring of lipid and contents release and estimation of SUV, lipid, and fusion pore properties[27]. The protocol starts with instructions for preparing the microfluidic cells, made by bonding a poly(dimethyl siloxane) (PDMS) elastomer block containing grooves with a glass coverslip[25]. Next, preparation of v-SUVs with both lipid and contents markers is explained. Sections 4 and 5 provide instructions for assembling the microfluidic cells, forming the SBLs *in situ* and checking for defects and fluidity, introduction of v-SUVs into the flow cells and detection of fusion events. Section 6 provides instructions for data analysis.

Protocol

1. Preparation of a PDMS Block to Form the Microfluidic Channel

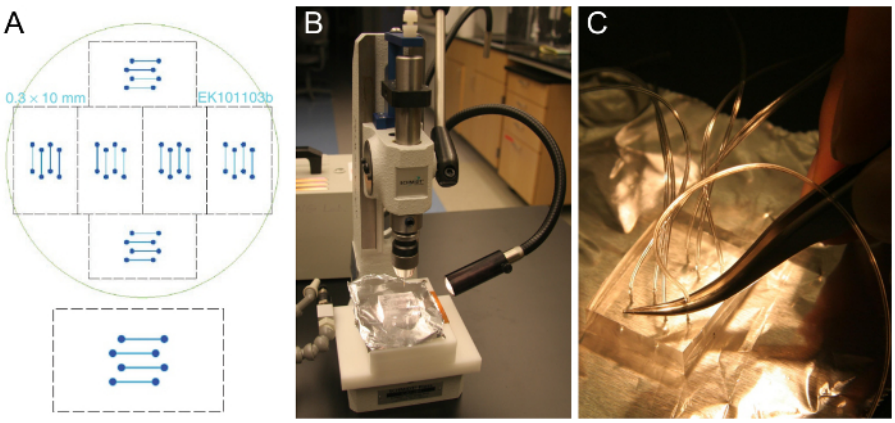

Figure 1. Microfabrication of flow cell template and PDMS block preparation. (**A**) Design of a four-channel flow cell that fits onto a 24 x 60 mm glass coverslip (bottom). Six identical designs are arranged to fit onto a 10 cm silicon wafer (top). (**B**) Cut out block of approximately 5-8 mm thick PDMS on a hole puncher. (**C**) Insertion of tubing into the punched hole using a pair of tweezers. Please click here to view a larger version of this figure.

1. Obtain a flow cell template such as the one in **Figure 1A**. Typical channels are 0.3-1 mm wide, 70-100 µm high, and 1-2 cm long. Fabricate a template using standard photolithography techniques in a cleanroom facility[25] or order if cleanroom access is not available. Alternatively, machine a template with larger dimensions from a suitable material.
   Note: Cleanroom staff can train and guide unexperienced users (access to a cleanroom facility is always restricted to users with proper training) in the design and ordering of a mask, wafer cleaning, and photolithography. Once a template is obtained, it can be used outside the cleanroom repeatedly, provided it is kept in a closed dish and care is taken to exclude dust.
2. Prepare a mixture of ~100 ml PDMS (silicone elastomer base) and ~10 ml of cross-linker (curing agent) in a disposable plastic cup. Break off the tip of a disposable pipette to handle the viscous PDMS more easily. Weigh the PDMS into the plastic cup as pipetting is not accurate.

3. Stir the mixture well. Remove the many air bubbles by degassing in a vacuum desiccator (about 20 min). As the cup is placed under vacuum, the bubbles will initially grow in size, increasing the volume of the mixture greatly. Control the vacuum that is applied and make sure the cup is deep enough to avoid a spill.
4. Pour a large drop of the degassed PDMS mixture into a glass Petri dish (150 mm x 20 mm) and press the wafer onto the PDMS with the template facing up. This avoids bubbles being trapped beneath the wafer. Trapped bubbles will expand and may tilt the wafer when the dish is placed in the oven. Now pour degassed PDMS onto the template on top of the wafer until it is covered by about 5-8 mm of PMDS. If an air bubble occurs gently remove it with a pipette tip.
5. Bake the PMDS in an oven at 60 °C for 3 hr. Ensure that the dish is level.
6. Use a new scalpel blade to cut out a PDMS block containing the molded channel structures. The cut out block needs to fit onto a coverslip (see step 4.1.9).
7. Peel out the cut out block from the dish and place it onto a piece of clean aluminum foil.
   Note: The cross-linked PMDS blocks can be kept for a few months. On a single wafer, there are 6 sets of flow channels (**Figure 1A**), so 6 PDMS blocks can be produced in a single PDMS molding. After cutting out all 6 of the PDMS blocks, clean loose pieces of PDMS, but otherwise do not remove the remaining PDMS before pouring and cross-linking the next batch, which will require only about half the PDMS used for the first batch. A good template can last a few years.
8. Use a hole puncher to drill through the PDMS block in one straight motion (**Figure 1B**). Start on the side of the channel grooves. Be sure to remove the punched out piece of PDMS. Repeat this for all eight holes of the four channel design.
9. Place the PDMS block channel side down onto a new and wrinkle-free piece of aluminum foil. Store the block for up to a few months in a dry box, ideally in a desiccator.
10. Push the tubing (0.25 mm ID, 0.76 mm OD) about one-third into the punched hole using a pair of tweezers (**Figure 1C**). Cut the tubing slanted for easier insertion. Leave tubes long enough to reach the SUV reservoir and the syringe pump, respectively. After placing the assembled chip onto the microscope, cut the tubes again if they are too long.
11. To connect to the syringes of the pump, cut a short piece of larger silicone tubing (0.51 mm ID, 2.1 mm OD) and insert the thinner tube into one side. This ready-to-use block of PDMS can be kept for a few months.

2. Coverslip Cleaning

1. Clean coverslips according to the protocol described in Karatekin and Rothman[25] using a strong oxidizing mixture of sulfuric acid (H_2SO_4) and hydrogen peroxide (H_2O_2). Perform this procedure in a cleanroom, and observe proper safety precautions. Alternatively, use a cleanroom cleaned coverslip that is commercially available (see Materials List).

3. Preparation of v-SUVS Containing Both Lipid and Content Labels

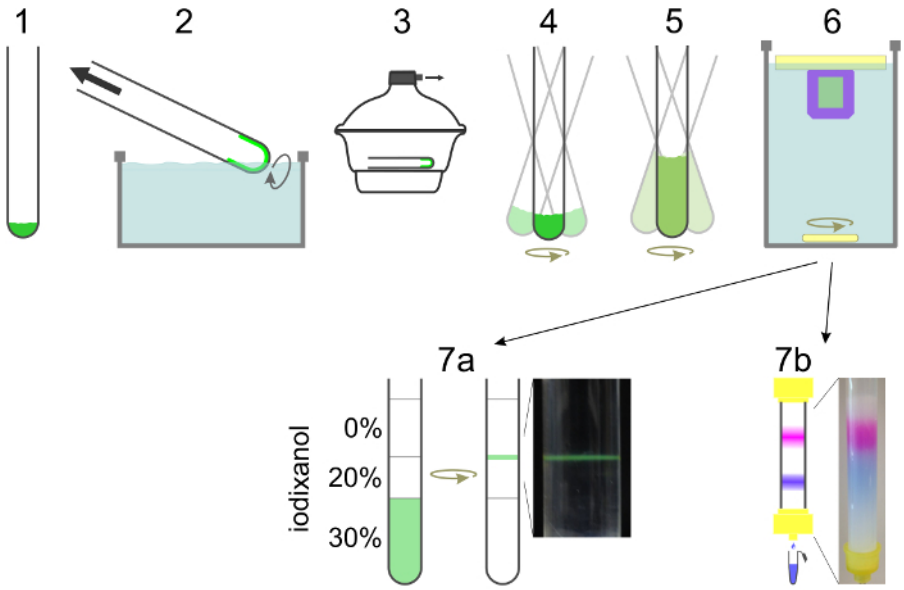

Figure 2. Schematic of SUV preparation. Lipids are mixed in a glass tube (1) and solvent is evaporated to form a lipid film by rotating the tube in a water bath (2). Remaining traces of solvent are removed under high vacuum (3). The lipid film is hydrated in reconstitution buffer containing detergent and protein while vortexed (4). If contents dye is to be encapsulated, it is included in this step as well as in the dilution step (5). Dilution of the detergent concentration below its critical micelle concentration leads to liposome formation. Detergent is dialyzed away overnight (6). For t-SUVs for SBL formation including NBD-PE (green), vesicles are floated in a density gradient and collected at the interface between two layers (7a). To separate v-SUVs with encapsulated content marker from free dye the sample is run over a size-exclusion column and collected in 0.5 ml fractions (7b). Please click here to view a larger version of this figure.

1. Prepare 4 L of reconstitution buffer, containing 25 mM HEPES-KOH, 140 mM KCl, 100 µM EGTA and 1 mM DTT, pH 7.4. Use most of the buffer for dialysis and 100 ml for other steps.

Note: Other buffers may be used, but it is important to keep the buffer osmolarity consistent throughout the experiment and choose conditions in which the proteins are functional. For preparing v-SUVs containing lipid labels only and t-SUVs, follow Karatekin and Rothman[25].

2. As lipid stocks are stored at -20 °C in chloroform or chloroform:methanol (2:1, v/v), let vials reach room temperature before opening to avoid condensation.
3. Rinse a glass tube with chloroform to remove trace amounts of detergent and mix the lipids at the desired ratio with a final amount of 1 µmol in a mixture of chloroform and methanol (2:1, v/v). Only use glass syringes/tubes to handle organic solvents/dissolved lipids.
   Note: The lipids used here are POPC:SAPE:DOPS:Cholesterol:PEG2000-DOPE:DiD at a molar ratio of 57.4:15:12:10:4.6:1 for v-SNARE containing vesicles and POPC:SAPE:DOPS:Cholesterol:brain PI(4,5)P_2:PEG2000-DOPE:NBD-PE (54.9:15:12:10:3:4.6:0.5) for t-SNARE SUVs. See Material for details. Other lipid compositions can be used.
4. Evaporate the solvent under a gentle stream of nitrogen, or in a rotary evaporator. Immerse the tip of the tube in a water bath (37 °C) heated above the highest melting temperature of the lipids to yield a homogenous lipid film and to avoid large changes in temperature while evaporating the solvent. Start vacuum at around 300 mbar until the lipid film is formed, then continue for ~2 min at highest possible vacuum in the rotary evaporator.
5. Remove the glass tube and wrap it in aluminum foil to avoid light exposure and remove remaining traces of solvent by placing the tube in a desiccator under high vacuum for at least 2 hr. This step can also run overnight.
6. To rehydrate the dried lipid film, prepare a mixture of detergent (n-Octyl-β-D-glucopyranoside, OG), protein (v-SNAREs), and SRB in reconstitution buffer (500 µl final volume). Keep the final detergent concentration ~2 times above the critical micelle concentration (CMC, 20-25 mM for OG) and adjust the final volume such that the detergent to lipid ratio is >10. Dissolve Sulforhodamine B (SRB) powder in the protein-detergent solution to obtain a final concentration of 10-50 mM SRB by gently shaking the solution. Adjust the osmolarity of the reconstitution buffer when adding high concentrations of SRB by reducing the concentration of potassium chloride accordingly.
   Note: Lipid-to-protein ratio (LP) for t-SNAREs is high (LP ~20,000, ~70 t-SNAREs per sq. micron[25]). Significantly higher t-SNARE densities in the SBL may lead to inactive protein aggregates with significantly reduced the fusion rates[17,24]. LP for v-SNAREs is much lower (LP ~200, ~7,000 v-SNAREs per µm^2), close to the v-SNARE densities found on synaptic vesicles[46,47]. To ensure protein function after recombinant expression and purification of v- and t-SNAREs it is useful to perform a simple bulk fusion assay[48] before going through all the steps of the single vesicle fusion assay.
7. Gently shake the pre-warmed glass tube containing the dried lipid film while adding the protein-detergent-SRB solution from step 3.6. Try to avoid creating bubbles. Continue to shake for 15 min at 37 °C.
8. Dilute the detergent fivefold by adding reconstitution buffer containing SRB (add 2 ml, 2.5 ml final volume) while rapidly vortexing to avoid concentration gradients. Continue to shake for 15 min to 1 hr at 37 °C.
   Note: Longer incubation increase protein reconstitution efficiency. The rapid dilution decreases the detergent concentration below the CMC and leads to the formation of small liposomes.
9. Dialyze the vesicle suspension first against ~1 L of reconstitution buffer for 1-2 hr at ambient temperature and then against 3 L of reconstitution buffer overnight at 4 °C with 4 g of polystyrene adsorbent, using a 20,000 MWCO dialysis tube or cassette. Use different beakers for dialysis of vesicles with and without SRB to prevent cross contamination.
10. Equilibrate a gel filtration column with reconstitution buffer. Run the vesicle suspension through the column to separate free SRB from the v-SUVs with encapsulated SRB. Use reconstitution buffer without SRB as eluent once the entire sample has entered the column. Collect v-SUVs in 0.5 ml fractions.
11. Verify successful SRB encapsulation at self-quenched concentrations by measuring SRB fluorescence before and after addition of detergent to an aliquot of vesicles[16]. Using a fluorescence spectrometer, excite the sample at 550 nm and scan the SRB emission between 570 nm and 630 nm. Expect a 4-8 fold increase in SRB fluorescence depending on the encapsulated amount upon detergent addition as the membrane is solubilized and the released SRB is diluted.
12. Characterize the lipid and protein recovery using fluorescence spectroscopy[24] and SDS-PAGE gel electrophoresis, respectively. Use a sensitive staining method, especially for the high LP t-SUV samples (see Materials List). Typically about 50% of both lipid and protein input is lost during the preparation resulting in a LP close to the nominal value.
13. Characterize SUV sizes using dynamic light scattering[24] or electron microscopy[48]. Store SRB containing v-SUVs at 4 °C up to ~3-4 days. Do not freeze, as freezing and thawing breaks the membrane and releases encapsulated SRB.

4. SUV-SBL Fusion Assay to Monitor Lipid Release Only

1. **Formation of the tethered supported bilayer within the microfluidic flow channels**
   1. Place the PDMS block (step 1.11) under high vacuum for at least 20 min prior to the experiment to remove dissolved gasses. This greatly reduces the risk of air bubbles in the microfluidic channels during the fusion experiment.
   2. Turn on the microscope setup and heat the stage and sample holder (**Figures 3** and **4**) to the desired temperature.
   3. Filter the reconstitution buffer used to dilute the vesicles through a filter with 0.45 µm or smaller pore size.
   4. Dilute ~30 µl of the NBD-PE labeled t-SUVs or protein-free (pf-SUVs) control liposomes (stock solution 0.5-1 mM lipid) with ~60 µl of buffer. The final concentration is not critical here.
   5. Degas this mixture using a 3 ml syringe. Press out most of the air above the sample while holding the syringe vertically. Seal the (needle free) tip using paraffin film and create a vacuum by pulling down the plunger. Tap the syringe barrel to accelerate degassing of the solution. Repeat this process a few times until no more bubbles occur when vacuum is applied.
   6. Use a hypodermic needle with a diameter slightly larger than the tubing that is attached to the PDMS block to punch a hole in the cap of a microcentrifuge tube. Make sure that the punched out piece of plastic is not inside the tube as it might clog the tubing connected to the microfluidic channel inlet later.
   7. Fill the degassed SUV solution into the microcentrifuge tube having a hole in the cap and place it into the holder on the microscope stage to equilibrate to the set temperature.
   8. Place a previously cleaned coverslip (section 2) in a plasma cleaner and run air plasma for about 5 min. Put the plasma treated coverslip (treated side facing up) on top of a few lint-free tissues serving as a cushion.

9. Remove the aluminum foil from the degassed PDMS block and place the block on top of the coverslip. When reusing the PDMS block put on and detach a piece of adhesive tape to the channel side to clean it. Press down the PDMS block onto the coverslip using a pair of tweezers to make it stick, but do not press too hard as the glass might break.
10. Place the assembled flow cell onto the microscope stage and connect the tubing to the SUV reservoir and the syringe pump, respectively. Tape the coverslip to the stage (**Figure 3B**).
11. Start aspirating SUVs at 3 µl/min until the solution fills the channels completely (~2.25 mm/sec for the 75 µm x 300 µm channel cross-section). When solutions for all channels start moving up the tubing on the exit side, reduce flow to 0.5 µl/min and incubate for 30-45 min.
    Note: The time between plasma treating the glass slide and flowing the SUVs into the channel should not exceed 10-20 min as the effect of the plasma treatment is transient.
12. Check the channels for any leak. Use a 10-20X air objective to observe NBD-PE fluorescence from the NBD-PE containing t- or pf-SUVs. Excite NBD fluorophores using the 488 nm laser. Leaks are difficult to detect using bright field illumination.
13. Put a tube with degassed reconstitution buffer into the holder and let the temperature equilibrate as fast changes in temperature might cause defects in the SBL. Stop the flow and wait ~1 min to make sure the flow has stopped completely and no air bubble will be aspirated into the tube before switching the inlet tubes to the degassed buffer.
14. Rinse all channels with degassed buffer to wash away unbound SUVs.
15. Switch to a higher magnification TIRF objective (60X, oil, NA 1.45-1.49) and verify that the bilayer looks homogeneous and is free of any obvious large-scale defects such as dark patches or lipid tubules extending out from the SBL.

2. **Check the fluidity of the bilayer**
    1. If a dedicated FRAP unit is not available, or if a FRAP sequence cannot be programmed, then qualitatively test membrane fluidity as follows.
        1. Close the field diaphragm to a small size (~40 µm diameter) and adjust the 488 nm excitation light intensity through the software (20-80 µW, or 15-60 nW/µm^2) to bleach the NBD-PE fluorescence in the exposed area significantly, but not completely. For a fluid bilayer, at steady state, the fluorescence intensity in the middle of the exposed area should be lower than at the edges, as intact NBD-PE molecules enter the exposed area and diffuse a certain distance before bleaching. In contrast, if the surface-adhered SUVs failed to burst, or for some other reason the supported bilayer is not fluid, all fluorophores in the exposed area should bleach.
            Note: Laser intensity values in this and later steps are given as a rough starting point and should be optimized for a given set of conditions.
        2. Stop the illumination and start it again a few minutes later to verify the results of the steady state measurements

    2. Program a FRAP sequence for a more quantitative measurement, if possible. See supplemental files and the corresponding legend for details.
        Note: Sometimes SUVs will adhere onto the glass coverslip, but fail to burst and form a fluid bilayer. If this occurs, rinse the channels with degassed reconstitution buffer containing 10 mM Mg^{2+} to help supported bilayer formation. Use fluorescence bleaching to assess bilayer fluidity as in 4.2. Once a fluid bilayer is formed, rinse with Mg^{2+}-free reconstitution buffer.

3. **Introducing v-SUVs into the microfluidic flow channels**
    1. Degas reconstitution buffer and use it to dilute the v-SUV stock solution by a factor of about 10^3 to 10^5 depending on the v-SUV stock concentration. Aim for a dilution that results in about 10-100 fusion events within 60 sec in the field of view.
        Note: Too many fusions increase the background fluorescence (since each event deposits LR-PE or DiD lipid labels into the SBL) and make detection and analysis of fusion events difficult. In contrast, a fusion rate that is too low results in poor statistics¸ or requires acquisition of many more movies. For a v-SUV concentration of 0.1 mM lipid, start by diluting 5 µl SUV stock in 995 µl reconstitution buffer and then dilute 5-50 µl of this in 950-995 µl reconstitution buffer.
    2. Let temperature equilibrate before stopping the flow and inserting the inlet tube into the diluted v-SUV solution.
    3. Adjust the TIRF angle and polarization as follows.
        1. After setting the desired polarization by rotating the excitation beam, adjust the tilt of the mirror commanding the position of the beam via a stepper motor through the software. Slowly move the position of the laser beam from the center of the objective at the back focal plane to one side off-center. Observe the light from the objective at the front side emerge with an increasing angle with respect to the objective axis as the position is moved further off-center.
        2. Note the motor position when the exiting beam first disappears into the objective, *i.e.*, when TIR is first achieved.
        3. Slowly keep moving the beam position further off-center while monitoring the fluorescence from the surface. Note the motor position when the surface fluorescence disappears when the beam has moved too far off-center.
        4. Choose a beam position between the two limits determined above. For best signal-to-noise ratio and more signal enhancement upon fusion, choose a shallow penetration depth (beam position closer to the edge of the objective) that still provides uniform illumination of the viewfield.
            Note: It is best to keep the same TIR beam position (same penetration depth) for all experiments after settings are optimized. Make sure rotating the polarization does not result in changes in beam position.

    4. Flow v-SUVs into the channel at a flow rate of 2 µl/min, corresponding to an average linear flow velocity of ~1.5 mm/sec for a cross section of 75 µm x 300 µm. Switch to the excitation/emission settings to monitor lipid mixing (LR or DiD only).

4. **Observing fusion between single v-SUVs and the SBL**

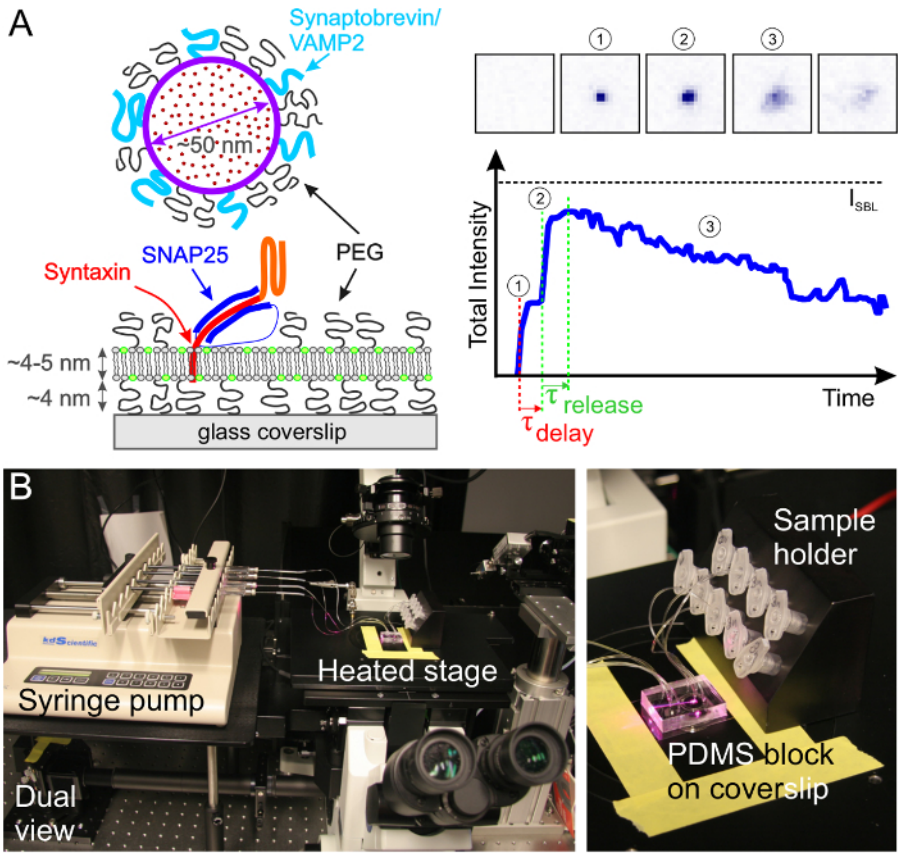

Figure 3. The experimental pTIRF setup. (**A**) Schematic representation of a v-SUV and a t-SBL on a glass substrate. False-color TIRFM images of single SUV-SBL fusion event showing lipid docking (1) and release of lipid dye into the SBL (2) followed by bleaching and decrease of the fluorescence intensity (3). The total fluorescence intensity (sum of pixel values in the 5.3 µm x 5.3 µm box) signal is shown. (**B**) The coverslip bonded to the PDMS block is taped onto the heated stage. Inlet tube for microfluidic channels draw samples from tube in metal sample holder (right) aspirated by the syringe pump (left). Beneath the pump is the dual emission unit. Please click here to view a larger version of this figure.

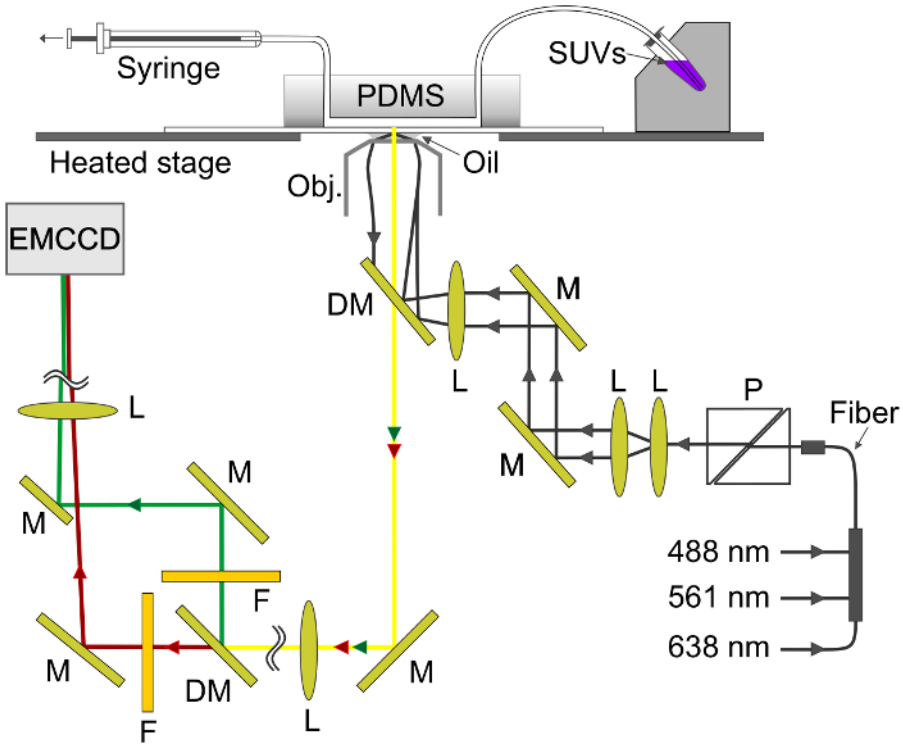

Figure 4. Schematic of the experimental setup. The evanescent wave is created at the glass-buffer interface in the microfluidic channel. The SBL is formed on the glass and v-SUV are aspirated from the metal sample holder (top right) through the channel into the syringe (top left). M, mirror; DM, dichroic mirror; L, lens; F, filter; P, polarizer. Please click here to view a larger version of this figure.

1. Continuously excite and monitor v-SUV fluorescence using a 561 nm (for LR-PE) or 638 nm (for DiD) laser depending on the fluorophore incorporated in v-SUVs. As v-SUVs reach the flow channel and dock onto and fuse with the SBL, the background fluorescence signal starts to accumulate.
2. Adjust the excitation laser intensity through the software to continuously bleach the background fluorescence such that at steady state new docking and fusion events can readily be observed.
   Note: If bleaching is too slow, background fluorescence will be too high. If bleaching is too fast, signals from docked SUVs and from fluorophores released into the SBL will fade rapidly, shortening the window during which fusion of docked SUVs can be detected or a fluorophore can be tracked. For LR-PE excited at 561 nm, 2.5-7.5 mW power illuminating a 190 µm diameter circle (100-250 nW/µm^2) is a reasonable value to start. For 638 nm excitation of DiD, 0.8-1.6 mW power over a 190 µm diameter circle (30-60 nW/µm^2) can be used for initial tests.
3. Acquire several movies at different positions in a given channel. Check NBD-PE fluorescence to verify that the SBL does not have defects at these positions. Acquire full-frame movies at the maximum rate (~50 frames/sec) or a cropped region of interest at higher frame rate (up to ~100 Hz) for 60 sec.
4. Move to another microfluidic channel and repeat the recordings for other conditions. Include negative controls such as a protein-free SBL or SUVs, add the soluble cytoplasmic domain of the v-SNARE VAMP2 (CDV) as an inhibitor or treat v-SUV with tetanus neurotoxin (30 min at 37 °C) in one or more of the channels on the same coverslip.

5. **Clean up and PDMS recycling**
   1. In order to reuse the PDMS block, rinse the microfluidic channels with ~200 µl of 70% ethanol at a flow rate of 5 µl/min. Finally, aspirate air through the tubing and channels.
   2. Detach the PDMS block gently from the coverslip by squeezing it slightly. Place it on a clean piece of aluminum foil. Store in a vacuum desiccator. It can be reused several times.
   3. For a more thorough cleaning rinse the channels with a detergent or sodium hydroxide solution prior to 70% ethanol. Alternatively, remove all tubes from the PDMS and sonicate the block for 30 min in isopropanol, before drying and inserting new tubing.

5. SUV-SBL Fusion Assay to Monitor Lipid and Content Release Simultaneously

1. For dual color monitoring of simultaneous lipid and soluble contents release, follow the same steps as in section 4, except use liposomes labeled with both a lipid (DiD) and a soluble contents (SRB) label, as explained in section 3. SRB is encapsulated at 10 mM and is initially highly self-quenched.
2. Using the configuration shown schematically in **Figure 4**, excite SRB and DiD fluorescence simultaneously using 561 nm and 638 nm lasers, respectively. A dichroic mirror (640 nm) splits the emission into two beams that run through a short (595/50 nm) and a long (700/75 nm) wavelength filter to detect the SRB and DiD emissions, respectively. The two emission beams are projected side-by-side onto the EM-CCD chip.

6. Data Analysis

1. **Analysis of FRAP data**
   1. Use the MATLAB program provided in the Supplementary Information to estimate the lipid diffusion coefficient, ***D***. The program reads a list of OME-TIFF files[49], detects the bleached area, plots the mean pixel values in the bleached area as a function of time, and fits the resulting recovery curve to a model by Soumpasis[50] to extract the recovery time, $\tau = w^2/(4D)$, where ***w*** is the radius of the bleached circle.
   Note: A MATLAB program was provided earlier[25] for analysis of FRAP movies using Nikon ND2 files. The current program reads OME-TIFF files[49], because most file formats can readily be converted to OME-TIFF. A quantitative analysis of FRAP data is easiest and most accurate when bleaching is instantaneous, the bleached region is a circle, and bleaching during read-out is negligible. Although these criteria are not strictly satisfied in the simple FRAP measurements described here, a reasonable estimate of the diffusion coefficient can be obtained. For a more accurate estimate, use tracking of single lipid dyes (section 6.3).

2. **Analysis of docking rate, fusion rate and docking-to-fusion delay times**
   1. Use ImageJ to open a movie to analyze and adjust brightness and contrast to clearly identify vesicle docking and fusing events. Start the SpeckleTrackerJ[26] plugin. See Smith *et al.*[26] and online documentation for SpeckleTrackerJ for instructions for usage.
   2. Identify all newly docked SUVs in SpeckleTrackerJ. To distinguish SUVs that dock tightly from those that bounce off the SBL, impose a minimum docking duration of a few frames. Save the tracks, and repeat for all movies.
   Note: For the docking rate, all that matters is to identify when a SUV docked, so only the first frame in which the SUVs docked needs to be recorded in these tracks. The rest of the tracks will not be taken into account in the analysis. However, auto-tracking each SUV until it bleaches or fuses helps mark SUVs that have already been tracked.
   3. Identify all fusing vesicles. For these, the tracks should include all frames from the first frame a SUV docked until the first frame in which fusion is evident by a sudden increase in the fluorescence of the tracked spot. The durations of these tracks are used to calculate the docking-to-fusion delays. Save all tracks. Repeat for all movies.
   4. For batch analysis of docking or fusion data, compile a list of trajectory files from the relevant movies and run the MATLAB programs provided with Karatekin and Rothman[25]. Follow instructions that are provided together with the programs.
   Note: The programs plot the cumulative docking and fusion events as a function of time, based on information extracted from the trajectory files. Docking and fusion rates are estimated from the slopes of these plots. For fusion data, the docking-to-fusion delays are also calculated and their distribution plotted as a survival plot, *i.e.*, the probability that fusion has not yet occurred by a given delay after docking.

3. **Lipid diffusivity**
   1. For each fusion event, track single fluorescent lipids as they become discernible when they have diffused sufficiently away from the fusion site (**Figure 6**). Use SpeckleTrackerJ for tracking, and save the tracks for further analysis using MATLAB. Depending on the size of the fusing vesicle, typically 3-30 single fluorophores can be tracked. Because longer tracks are desirable for the calculation of D_{lip}, try to track single molecules as long as possible, using manual correction of trajectories if necessary.
   2. Calculate the mean squared displacement (MSD) for single lipid marker trajectories that last > 40-50 frames (about ~1.5 sec). Use the MSD to calculate the lipid diffusion coefficient, D_{lip}. See Smith *et al.*[26] and Stratton *et al.*[27] for details.

4. **Single lipid dye intensity, SUV-SBL intensity reduction factor, and vesicle size**
   1. Measure the sum of pixel values of a lipid marker in a 3 x 3 pixel (0.8 µm x 0.8 µm) area around the marker for ~15 frames before and after the marker bleaches in a single step. Subtract the background intensity averaged over the post-bleach frames from the pre-bleach intensity averaged before bleaching to obtain the intensity of the tracked lipid marker. Repeat the measurement for as many markers as practical for a given movie.
   2. Plot the distribution of single lipid label intensities, I_{lip}, and fit a Gaussian to estimate the mean.
   3. Calculate the delay between when fusion occurred and when the trajectory of a single lipid marker released in that event ended in a single-step bleaching. Obtain the bleaching time for a fluorophore in the SBL, τ_{bleach}, by plotting the survivor function of the delays and fitting to an exponential.
   Note: Because the polarized excitation field couples more weakly to the fluorophores on a SUV, the bleaching time of a SUV is usually much slower[27].
   4. Estimate λ_{TIRF}, the intensity reduction factor for a lipid dye when in the SUV relative to when it is in the SBL, following Stratton[27] ($\lambda_{TIRF} I_{lip}$ is the intensity of a single dye in the SUV).
   Note: If bleaching were negligible, λ_{TIRF} would be equal to the docked intensity I_{dock} (point (1) in **Figure 3A**, right panel), divided by the total intensity reached after all fluorophores are deposited into the SBL upon fusion (dashed line labeled I_{SBL} in **Figure 3**). However, due to rapid bleaching in the SBL, I_{SBL} is typically not reached and an accurate estimate of λ_{TIRF} requires fitting the release kinetics to an expression[27] that includes both τ_{bleach} (see 6.4.3) and λ_{TIRF}. Separate expressions are provided in Stratton *et al.*[27] for the cases of pore-limited and diffusion limited release kinetics; the best fit case varies from event to event (see 6.5.1 for the case of pore-limited kinetics).
   5. Calculate the vesicle area for individual events from[27] $A_{ves} = I_{dock}/(\lambda_{TIRF}\, I_{lip}\, 2\, \rho_{lip})$, where I_{dock} is the docked SUV intensity, I_{lip} is the mean intensity of a single lipid dye in the SBL, λ_{TIRF} is the intensity reduction factor for a lipid dye when it is in the SUV relative to when it is in the SBL, and ρ_{lip} is the known areal density of lipid dyes.

5. **Fusion pore properties**

1. Assuming release is pore-limited, fit the lipid label release kinetics to [27] $\frac{I_{tot}(t)}{I_{fus}} = e^{-t/\tau_{release}} + \frac{\left(e^{-t/\tau_{bleach}} - e^{-t/\tau_{release}}\right)}{\lambda_{TIRF}\,(1-\tau_{release}/\tau_{bleach})}$, where I_{fus} is the docked SUV intensity just before fusion and the other parameters are as defined earlier. Use the value of τ_{bleach} obtained in 6.4.3 as a fixed parameter, and extract the best fit estimates for λ_{TIRF} and $\tau_{release}$.
2. Estimate the fraction of time the pore is open, P_0, assuming retardation of lipid release is due to pore flickering[27]: $P_o = A_{ves}\ b/(2\pi\ r_p\ \ D_{lip}\ \tau_{release}) = (\tau_{ves}/\tau_{release})(b/(2\pi\ r_p))$, where A_{ves} is the vesicle area (section 6.4.5), b is the pore height (typically taken to be ~15 nm), $r_p \approx 3$ nm is the effective pore radius as seen by the diffusing lipid labels and includes half the bilayer thickness (~2 nm), D_{lip} is the lipid diffusivity (calculated in 6.3), and $\tau_{release}$ is the time for the lipids to be released from the SUV into the SBL (from 6.5.1).
3. To confirm that a nominal $P_0 > 1$ indicates a fully open pore, $P_0 = 1$, fit the intensity time course to equation 4 of Stratton *et al.*[27], the predicted kinetics for a permanently open pore. This fit should be better than fitting the expression in 6.5.1 for a permanently open pore.

Representative Results

SBL Quality

It is crucial to verify the quality and fluidity of the SBL prior to the fusion experiment. The fluorescence at the bottom, glass side of a microfluidic channel should be uniform, without any obvious defects. If an air bubble passes though the channel, it usually leaves visible scars on the SBL. If there are such large scale scars/defects, do not use that channel. Sometimes SUVs may adhere onto the substrate but fail to burst and form a continuous SBL. If that is the case, the fluorescence may still appear very uniform, but will not recover after bleaching a small region. Introducing 10 mM Mg^{2+} often helps solving this issue. Other agents can be introduced to help bursting the SUVs, such as other divalent cations[51], a polymer solution[52], or osmotic shock[25].

Even when fluorescence is largely homogeneous and it recovers after bleaching, some unfused SUVs may remain intact on the surface. Such a liposome will appear as a bright spot if it is sufficiently large. After bleaching a region containing such liposomes, the previously bright spots turn dark and remains so, as the fluorescence recovers in the surrounding SBL, but not in the intact liposomes. Such intact liposomes do not affect fusion measurements, provided their density is low.

Temperature changes result in changes of SBL area because the mean area occupied by a lipid depends on temperature. Increasing the temperature or decreasing it by 5-10 °C or more can result in excess area going into tubes extruded from the surface, or dark, SBL-free spots appearing on the surface, respectively[53]. It is therefore important to keep temperature variations to a minimum.

A typical FRAP measurement is shown in **Figure 5** for an SBL that was relatively defect-free and fluid.

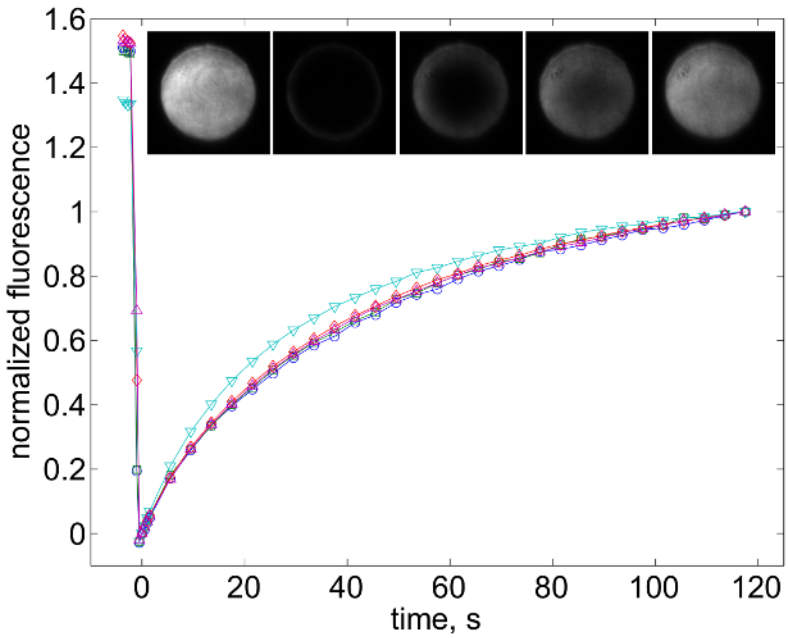

Figure 5. FRAP to examine SBL fluidity. A sequence of images showing an illuminated area delimited by the closed field diaphragm (diameter 49 µm) before (first frame) and after bleaching with a strong light pulse. The area is imaged at low light exposure to follow the fluorescence recovery by diffusion of NBD labeled lipids. The graph shows the normalized fluorescence as a function of time for several channels from different coverslips indicating the high level of reproducibility of the method. The Lipid composition of the t-SBL was POPC:SAPE:DOPS:Cholesterol:brain PI(4,5)P_2:PEG2000-DOPE:NBD-PE (54.9:15:12:10:3:4.6:0.5 mole %) and LP=20,000. The bleach

area was **984.203** μm^3. The recovery time and the diffusion coefficient calculated from a fit (see 6.1) were ***τ* = 67.3** sec and ***D* = 1.99** μm^2/sec, respectively. Please click here to view a larger version of this figure.

Single-color Detection of Docking and Fusion Events Using a Lipid Label

Manual counting of docking and fusion events is a tedious task as 100-400 events per condition are needed for good statistics. Since SUVs can move on the SBL before fusing, a tracking software is needed. SpeckleTrackerJ[26] plugin for ImageJ has features that were specifically developed for tracking SUVs for analysis of docking and fusion events. Often only a fraction of docked vesicles end up fusing; to calculate the docking rate many more SUVs need to be tracked than those that fuse or only a portion of the movie needs to be analyzed until a sufficient number of events are detected for a reliable estimation. If the main focus is the fusion rate and/or the docking-to-fusion delays, only the fusing SUVs need to be identified and tracked.

After ensuring the quality of the SBL, SUVs are introduced into the channels and their fluorescence is continuously excited under TIR using s-polarized light. For the initial experiments, the incidence angle of the TIR excitation beam may need to be adjusted to tune the penetration depth of the resulting evanescent wave. A representative single SUV docking and fusion event is shown in **Figure 6A**. The vesicle docked during the frame marked D and fusion started in frame F. About 1.3 sec later (frame S) single lipids became discernible as they diffused away from the fusion site. The total fluorescence intensity (sum of pixel values) in each box is plotted as a function of time in **Figure 6B**, with the frames at which docking and fusion occurred indicated. The cumulative number of fusion events as a function of time is plotted in **Figure 6C**, for five different movies using t-SNARE reconstituted SBLs (t-SBL, LP=20,000, about 70 t-SNAREs per sq. micron). The fusion rate from each movie was calculated from a linear fit to the slope. This average fusion rate ± SEM is shown as a bar graph in panel D. The docking-to-fusion delay for the example shown in **Figure 6A**, **B**, was 0.07 sec. The distribution of delays calculated similarly for a total of 158 events is shown in **Figure 6D** as a survivor plot, *i.e.,* the probability that a docked vesicle has not yet fused by a given delay. About 1/2 of these vesicles fused within 100 msec. With increasing cholesterol levels, the distribution of docking-to-fusion delays shortens, even though lipid diffusion slows[27].

It is important to run control experiments in parallel. On the same coverslip from which the data in **Figure 6B**, **D** were acquired, control conditions were tested in neighboring channels. In one channel, the SBL did not include any t-SNAREs. Out of 5 movies lasting 60 sec each, only 7 fusion events were recorded compared to 158 when the t-SNAREs were included (**Figure 6C**). In another channel, the soluble cytoplasmic domain of the v-SNARE VAMP2 (CDV) was included. CDV binds the t-SNAREs on the SBL, preventing binding of the full-length VAMP2 that is on the SUVs. In five 60 sec movies, no fusion events were detected in the presence of CDV (**Figure 6C**).

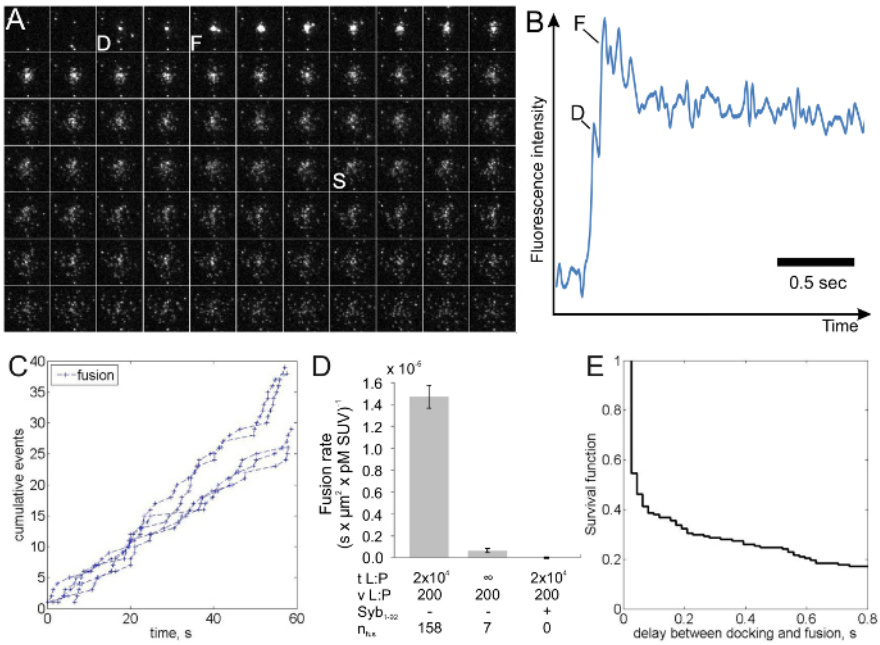

Figure 6. SUV-SBL docking and fusion events. (**A**) Sequence of images of a v-SUV fusion event with the t-SBL imaged by pTIRF microscopy following the spreading of LR-PE. Images are taken every 18 msec, only every second frame is shown. D and F mark the onset of docking and fusion, respectively. Individual lipid labels become identifiable as they diffuse away from the fusion site and one another (S). Frame dimensions: 16.7 μm x 16.7 μm. (**B**) Fluorescence intensity as a function of time for the fusion event shown in (A). (**C**) Cumulative number of fusion events as a function of time for v-SUVs labeled with DiD from another set of experiments. (**D**) the normalized fusion rate (mean ± SEM, s x μm^2 x pM SUV)$^{-1}$, assuming 2 x 10^4 lipids per SUV and (**E**) the survival probability for a given time after docking of the vesicle. The composition for all SBLs were POPC:SAPE:DOPS:Cholesterol:brain PI(4,5)P_2:PEG2000-DOPE:NBD-PE (54.9:15:12:10:3:4.6:0.5 mole %) and LP=20,000. v-SUVs were composed of POPC:SAPE:DOPS:Cholesterol:PEG2000-DOPE:LR-PE (57.4:15:12:10:4.6:1 mole %) and LP=200 for A and B. For C-E, the v-SUV composition was similar, except DiD was used instead of LR-PE. Please click here to view a larger version of this figure.

Lipid Diffusivity, Vesicle Size, and Fusion Pore Properties

The single-molecule sensitivity of the assay allows extraction of several parameters in addition to the docking and fusion rates and the docking-to-fusion delay distributions. Single, fluorescently labeled lipids become discernible as they diffuse away from the fusion site (**Figure 6A**). Tracking these directly provides lipid diffusivity[26], D_{lip}, and a digital measurement of the bleaching rate for fluorophores in the SBL[27]. As mentioned in Introduction, the fluorescence emission of the labels differ in the SUV *versus* in the SBL, due to three factors that are in general difficult to disentangle: (i) dequenching of labels upon fusion, due to their dilution when transferred into the SBL, (ii) a higher excitation intensity in the SBL due to the decay of the evanescent field generated by TIR, and (iii) the orientation of the fluorophore transition dipoles with respect to the polarization of the excitation beam. The magnitude of factor (ii) depends on the relative sizes of the evanescent field decay length and vesicle size and is different for every fusion event due to the dispersity in SUV sizes. Factor (iii) depends on the fluorophore and the polarization used. Rather than trying to disentangle these effects, one can measure the magnitude of the fluorescence change directly by comparing the total pixel values in a region surrounding a SUV before fusion and after all fluorophores have been deposited into the SBL following fusion (**Figure 3A**, (1) vs. (2)). Unlike in previous work[29,44], the region should be chosen sufficiently large so that no fluorophores will have left it via diffusion for the times considered after fusion. Choosing a 30 x 30 pixel region (8 µm x 8 µm) for analysis up to 1.6 sec after fusion is usually adequate[27]. Ignoring bleaching for the moment, the ratio of I_{tot} before and after fusion provides the fluorescence intensity reduction factor, λ_{TIRF}. The vesicle size can be estimated given the fluorescence intensity of a single label in the SBL (I_{lip}), the factor by which its intensity would be reduced if it were in a SUV (λ_{TIRF}), the known density of labels in the SUV, and the area occupied by a lipid. In practice, bleaching is usually fast enough that by the time all markers are deposited into the SBL, some have already bleached. For this reason, for an accurate estimation, the fluorescence intensity reduction factor, λ_{TIRF}, and the lipid release time, $\tau_{release}$, are best extracted from a fit to the time course of the total pixel values that takes into account bleaching[27]. The bleaching rate of labels in the SBL is independently estimated from single lipid dye tracking, or by fitting an exponential to the total intensity profile, I_{lip}, at long times (*e.g.,* regime (3) in **Figure 3**). Knowing the size of a fusing vesicle and lipid diffusivity allows comparison of the actual lipid release time, $\tau_{release}$, to the diffusion time of a lipid around the vesicle $\tau_{ves} = A_{ves}/D_{lip}$, where A_{ves} is the vesicle area and D_{lip} is the lipid diffusivity. If the two time scales are comparable, the pore presents little resistance to lipid release, and release is diffusion-limited. In contrast, if $\tau_{release} \gg \tau_{ves}$, then the pore significantly retards lipid flux. A quantitative measure of the retardation is the "pore openness", P_0, equal to the ratio $\tau_{ves}/\tau_{release}$ times a factor of order unity related to pore geometry[27]. For a two-state, open/closed pore, P_0 is the fraction of time in the open state. For a flickering pore whose size continuously varies, P_0 represents the time-averaged radius relative to the fully open radius.

The signal-to-noise ratio needs to be sufficiently good for tracking single lipid fluorophores. This is more easily achieved in single-color experiments, using a bright marker such as LR-PE.

Simultaneous Detection of Lipid and Soluble Cargo Release

A representative event is shown in **Figure 7**. At the high concentrations used for encapsulation, the SRB fluorescence is initially self-quenched. Therefore, most docked v-SUVs are only detectable by their DiD signal[27]. A sharp increase in DiD fluorescence marks lipid mixing, as in single-color lipid-label experiments. The onset of lipid release coincided with the onset of an increase in SRB fluorescence. This increase was most likely due to SRB dequenching as the SRB molecules escaped the SUV and the remaining SRB was diluted to below self-quenching concentrations. Interestingly, the SRB fluorescence reached a stable plateau. If the fusion pore remained open, one would expect the SRB signal to increase to a maximum due to dequenching, followed by a decrease to background as the remaining SRB left the SUV, or if the SUV collapsed into the SBL. The stable plateau most likely indicates the pore resealed after releasing all lipid labels and a fraction of the soluble cargo.

In some cases, the lipid release signal was not accompanied by any detectable contents release signals. This could be either because the pores were too small to allow passage of SRB, or somehow the SUV had already lost its soluble cargo. To distinguish between these two possibilities, bleaching of docked SUVs can be analyzed. Bleaching of the lipid label DiD reduces its fluorescence signal within seconds, whereas bleaching of the initially self-quenched SRB results in an increase of the SRB signal as a fraction of the SRB are photo-converted to other products and self-quenching is relieved. While most docked SUVs (48 out of 58 analyzed events) displayed the expected increase in SRB fluorescence over extended periods of illumination, a small fraction (10/58) did not show any SRB signals at all. Thus, a small fraction of the SUVs may lose their soluble content during the period between their preparation and use in the experiments.

In more than 80% of events (74 out of 91) for which both SRB and DiD signals could be followed, the SRB fluorescence increased and remained at a stable plateau[27]. In ~20% of these cases the remaining SRB fluorescence was suddenly released up to a few seconds later. This might either be due to a reopening of the pore allowing rapid, full release within 1-2 frames (18-36 msec) or a bursting of the SUV due to accumulated photo-damage[16]. Whatever its origin, this second, rapid release of SRB rules out the possibility that the residual SRB signal after the initial release might be due to the SRB remaining entrapped in the space between the SBL and the glass substrate after full release. Such a mechanism was suggested in an earlier study where the SBL was supported directly on glass, with little space between the two[16]. In contrast, the PEGylated lipids used in this assay should provide 4-5 nm of space between the SBL and the glass[25], allowing the SRB to diffuse away from the fusion site.

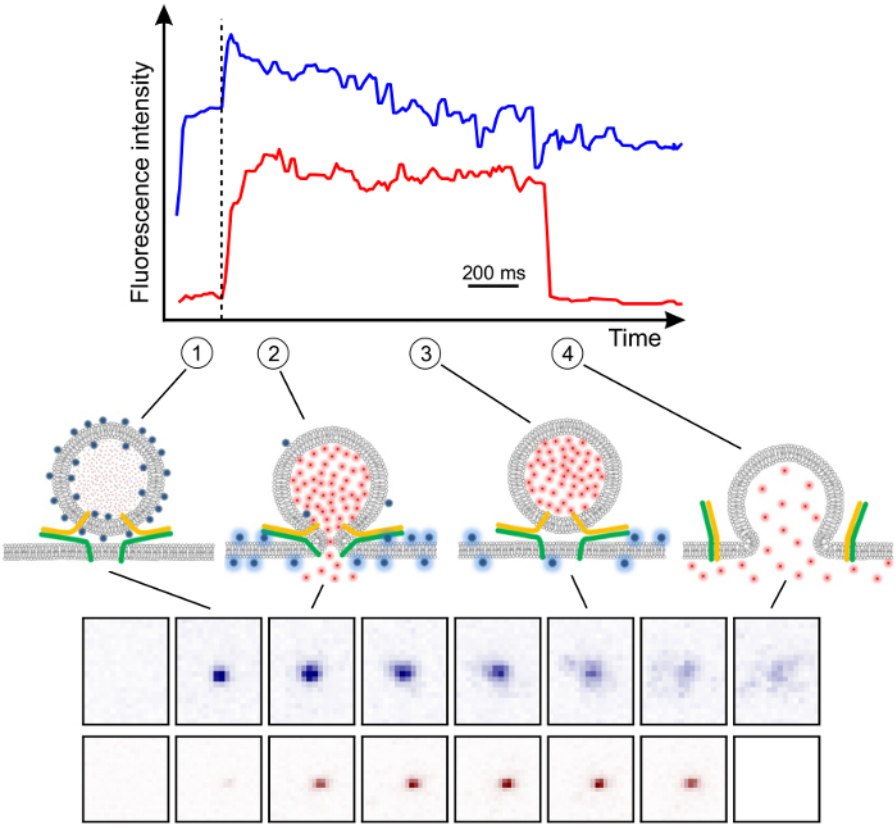

Figure 7. Simultaneous lipid and content release. Fluorescence signals from lipid (blue) and content (red) marker for a SUV-SBL fusion event (for details see text). Snapshots from each channel are shown at the bottom (4.0 µm wide). Cartoons (middle) illustrate the different stages. (1) SUV docks, DiD fluorescence is low. (2) Fusion allows transfer of DiD into the SBL and DiD fluorescence increases. SRB signal also increases as self-quenching is relieved by escape of SRB through the pore. (3) SRB signal remains stable while DiD molecules diffuse within the SBL indicating a possible resealing of the pore. (4) SRB signals decrease very rapidly, due to rapid full fusion or liposome bursting. The composition of v-SUVs was POPC:SAPE:DOPS:PEG2000-DOPE:DiD (67:15:12:5:1 mole %), LP 200, while t-SBLs were composed of POPC:SAPE:DOPS:brain PI(4,5)P_2:PEG2000-DOPE:NBD-PE (64.5:15:12:3:5:0.5 mole %) and LP=20,000. Please click here to view a larger version of this figure.

FRAP_instructions.pdf - Instructions for setting up a FRAP sequence. Please click here to download this file.

ReadMe_FRAP.txt - text file describing the procedure to analyze FRAP recovery data using the MatLab code that is provided. Please click here to download this file.

EK_FRAPbatch.m - MATLAB file to batch-analyze fluorescence recovery after photobleaching. This file calls the MATLAB subroutines EK_getFRAPvals.m and EK_SoumpassisFit.m. Please click here to download this file.

EK_getFRAPvals.m - MATLAB file, subroutine called by EK_FRAPbatch.m. Please click here to download this file.

EK_SoumpassisFit.m - MATLAB file, subroutine called by EK_FRAPbatch.m. Please click here to download this file.

JN150923c1_FRAP_list.txt - An example of a list of filenames to be batch-analyzed by the main MATLAB script EK_FRAPbatch.m. Please click here to download this file.

The following files are TIF stacks and the corresponding text files for five examples of FRAP sequences that can be analyzed by running EK_FRAPbatch.m and choosing the JN150923c1_FRAP_list.txt file when prompted to choose a file list.

JN150923c1_F1_MMStack_Pos0.ome.tif - FRAP image stack. Please click here to download this file.

JN150923c1_F1_MMStack_Pos0_metadata.txt - corresponding text file with metadata. Please click here to download this file.

JN150923c1_F2_MMStack_Pos0.ome.tif - FRAP image stack. Please click here to download this file.

JN150923c1_F2_MMStack_Pos0_metadata.txt - corresponding text file with metadata. Please click here to download this file.

JN150923c1_F3_MMStack_Pos0.ome.tif - FRAP image stack. Please click here to download this file.

JN150923c1_F3_MMStack_Pos0_metadata.txt - corresponding text file with metadata. Please click here to download this file.

JN150923c1_F4_MMStack_Pos0.ome.tif - FRAP image stack. Please click here to download this file.

JN150923c1_F4_MMStack_Pos0_metadata.txt - corresponding text file with metadata. Please click here to download this file.

JN150923c1_F5_MMStack_Pos0.ome.tif - FRAP image stack. Please click here to download this file.

JN150923c1_F5_MMStack_Pos0_metadata.txt - corresponding text file with metadata. Please click here to download this file.

Discussion

Successful implementation of the SUV-SBL fusion assay described here depends critically on several key steps, such as functional reconstitution of proteins into liposomes, obtaining good quality SBLs, and choosing the right imaging parameters to detect single molecules. Although it may take some time and effort to succeed, once the assay is implemented successfully, it provides a wealth of information about the fusion process not available from any other *in vitro* fusion assay discussed in Introduction. The rates at which SUVs dock onto and fuse with the SBL, the distribution of docking-to-fusion times, lipid diffusivity, the size of every fusing liposome, and whether lipid release for a given fusion event is diffusion- or pore-controlled can be determined. If release is much slower than expected from diffusion, a model that assumes pore flickering underlies the retardation of lipid release yields, P_0 , the fraction of time the pore is open during fusion[27].

Previous work probing single SUV-SUV fusion[18-20,28] or fusion of liposomes and viral particles to SBLs[15-17,21,22,33,44] relied on FRET and self-quenching between dye molecules. In contrast, we largely avoid dye dequenching to probe kinetics of lipid label transfer into the SBL, for two reasons. First, FRET efficiency is a highly non-linear reporter of lipid release. Small changes in the inter-dye distance d result in large changes in FRET efficiency, but only for a limited range of d/R_0 values, where R_0 is the Forster distance. That is, a lag time between actual dye dilution and an observed increase in the dequenching signal may occur, due to the time required for to drop to a value close to R_0. Similarly, there is little change in the dequenching signal once the dye density decreases sufficiently upon lipid release such that $d/R_0 \gtrsim 1.4$, even if a significant amount of dye still remains in the vesicle. These properties make dequenching a good tool to obtain a spike in the signal to detect fusion events, but complicate quantitative kinetic analysis of lipid release using high time resolution. In contrast, changes in intensity due to dipole reorientation and evanescent field effects as a fluorophore transfers from a SUV into the SBL are linearly related to the fraction of dye still remaining in the SUV. Second, high concentrations of lipid labels required for self-quenching may affect the fusion process itself.

For polarized TIRF excitation, a home-built setup as in **Figure 4** is cost-effective and provides excellent control over polarization properties. However, a home-built setup is not necessary, as at least some commercial TIRF microscopes use polarized excitation and off-the-shelf two-color emission splitting modules are available. A commercial microscope that uses a polarization-maintaining (PM) fiber to couple the polarized excitation light emerging from the laser into the microscope was successfully used previously[25-27]. On such an instrument, the polarization can be rotated simply by rotating the PM fiber input to the microscope's TIRF unit. In contrast, some other commercial setups may employ a polarizing beam-splitter in the TIRF unit, making polarization adjustments more difficult or impossible. Unfortunately, polarization properties are often not specified for commercial systems. Thus, it is critical for users who do not want to construct a home-built system to discuss polarization properties and to try a demo unit before investing in a particular commercial option.

Simultaneous monitoring of lipid and soluble cargo release provides further information on the fusion process. Many pores seem to reseal after releasing only a fraction of the soluble label encapsulated into a SUV[27]. Usually all the lipid labels are released by the time the pore reseals, so pore resealing was not suspected previously from monitoring lipid release alone. Indeed, monitoring lipid release alone, Kiessling *et al.*[29] had suggested transfer of labeled lipids into the SBL occurred via extremely rapid collapse of the entire SUV membrane into the SBL.

Resealing of fusion pores after partial release of contents was previously observed in a liposome-tethered bilayer patch fusion assay. Rawle *et al.*[54] prepared freestanding bilayer patches that were tethered onto a coverslip by ~8 nm long DNA spacers. They then introduced liposomes whose fusion to the bilayer patch was driven by hybridization of complementary single-stranded DNA-lipid conjugates anchored to the liposome and patch membranes. 12% of all events were transient fusions, resulting in partial release of the liposome contents. Liposome bursting events, seen in some previous SUV-SBL fusion assays[44], were very rare. The authors suggested the ~8 nm space below the bilayer patch, preventing bilayer-substrate interactions, may have allowed non-leaky transfer of the liposome contents to the space below the bilayer. In addition, diffusion of the released soluble labels was not significantly hindered in the space between the planar bilayer and the glass substrate. In the assay described here, the planar bilayer is similarly kept ~5 nm away from the coverslip by the presence of poly(ethylene glycol)-lipid conjugates.

The additional information provided by two-color monitoring of soluble and lipid cargo comes with some trade-offs. First, preparation of SUVs with the two labels is somewhat more involved than including lipid labels alone. Second, there is some inevitable loss of signal-to-noise when monitoring signals from the lipid labels at the same acquisition rate as in single-color lipid release experiments (15-20 msec per frame). Some of this loss is due to the fact that DiD, used as a lipid label together with the soluble SRB marker, is not as bright as LR-PE used in single-color experiments. Additional losses result from higher background due to simultaneous two-laser excitation and additional components in the optical path (**Figure 4**). So far, the lower signal-to-noise prevented us from reliable tracking of single DiD labels in two-color experiments. This in turn prevented a thorough analysis to extract all the information that can be with single-color LR-PE measurements. This challenge may be overcome in the future by optimizing acquisition conditions and testing other pairs of compatible labels with improved properties.

Simultaneous monitoring of soluble and lipid cargo release can also detect hemifusion, a state in which the proximal leaflets have fused, but the distal leaflets have not. Indeed, such two-color experiments may provide the only conclusive assessment of the presence of hemifusion in other *in vitro* fusion assays[18,20]. However, hemifusion can reliably be detected in single-color SUV-SBL experiments monitoring lipid release alone[22,44]. In such experiments, about 1/2 the initial lipid label intensity of a SUV remains at the fusion spot. The remaining intensity may disappear when the distal leaflets fuse some time later, if the spot has not yet bleached.

Use of PEGylated lipids to introduce a soft cushion between the SBL and the glass support has been key in reproducing the SNAP25 requirement of exocytosis. The protocol results in a PEG brush covering the side of the SBL that faces the flow channel as well. This has some benefits, such as reducing non-specific interactions between SUVs and the SBL, as explained in Introduction. If proteins that interact with the

phospholipids of the SBL are introduced into the assay, however, the PEG brush will present a steric barrier against such interactions. Thus, for some applications, it would be desirable to include the PEG layer asymmetrically, only between the SBL and the glass coverslip. The side of the SBL facing the flow channel would then be able to interact with phospholipid binding proteins, such as synaptotagmin. This can be accomplished by using bi-functional PEG chains that can be covalently linked to the coverslip at one end and carrying a lipid anchor at the other. Langmuir-Blodgett methods can then be used to deposit a lipid monolayer onto the PEG layer[55]. Liposomes introduced above this hydrophobic surface fuse with it, forming a bilayer[56]. It is hoped that this approach will be combined with microfluidics in the future.

It is expected that the SUV-SBL assay presented here will be helpful in exploring the role of additional proteins that interact with SNAREs, such as the Munc18/Sec1 family, the calcium sensor synaptotagmin-1, and complexin.

Disclosures

The authors declare that they have no competing financial interests.

Acknowledgements

We thank Vladimir Polejaev (Yale West Campus Imaging Core) for the design and construction of the polarized TIRF microscope, David Baddeley (Yale University) for help with two-color detection instrumentation, and James E. Rothman (Yale University) and Ben O'Shaughnessy (Columbia University) and members of their groups for stimulating discussions. EK is supported by a Kavli Neuroscience Scholar Award from the Kavli Foundation and NIH grant 1R01GM108954.

References

1. Sudhof, T. C., & Rothman, J. E. Membrane fusion: grappling with SNARE and SM proteins. *Science*. **323**, 474-477 (2009).
2. Wickner, W., & Schekman, R. Membrane fusion. *Nat Struct Mol Biol*. **15**, 658-664 (2008).
3. Harrison, S. C. Viral membrane fusion. *Nat Struct Mol Biol*. **15**, 690-698 (2008).
4. Jahn, R., & Scheller, R. H. SNAREs--engines for membrane fusion. *Nat Rev Mol Cell Biol*. **7**, 631-643 (2006).
5. Lindau, M., & Alvarez de Toledo, G. The fusion pore. *Biochim Biophys Acta*. **1641**, 167-173 (2003).
6. Staal, R. G., Mosharov, E. V., & Sulzer, D. Dopamine neurons release transmitter via a flickering fusion pore. *Nat Neurosci*. **7**, 341-346 (2004).
7. Wu, Z. *et al.* Nanodisc-cell fusion: Control of fusion pore nucleation and lifetimes by SNARE protein transmembrane domains. *Sci. Rep.* **6**, 27287 (2016).
8. Alabi, A. A., & Tsien, R. W. Perspectives on kiss-and-run: role in exocytosis, endocytosis, and neurotransmission. *Ann Rev Physiol*. **75**, 393-422 (2013).
9. Rossetto, O., Pirazzini, M., & Montecucco, C. Botulinum neurotoxins: genetic, structural and mechanistic insights. *Nature Rev Microbiol*. **12**, 535-549 (2014).
10. Weber, T. *et al.* SNAREpins: minimal machinery for membrane fusion. *Cell*. **92**, 759-772 (1998).
11. Nickel, W. *et al.* Content mixing and membrane integrity during membrane fusion driven by pairing of isolated v-SNAREs and t-SNAREs. *Proc Natl Acad Sci U S A*. **96**, 12571-12576 (1999).
12. McNew, J. A. *et al.* Compartmental specificity of cellular membrane fusion encoded in SNARE proteins. *Nature*. **407**, 153-159 (2000).
13. Melia, T. J., You, D. Q., Tareste, D. C., & Rothman, J. E. Lipidic antagonists to SNARE-mediated fusion. *J Biol Chem*. **281**, 29597-29605 (2006).
14. Hernandez, J. M. *et al.* Membrane fusion intermediates via directional and full assembly of the SNARE complex. *Science*. **336**, 1581-1584 (2012).
15. Fix, M. *et al.* Imaging single membrane fusion events mediated by SNARE proteins. *Proc Natl Acad Sci U S A*. **101**, 7311-7316 (2004).
16. Bowen, M. E., Weninger, K., Brunger, A. T., & Chu, S. Single molecule observation of liposome-bilayer fusion thermally induced by soluble N-ethyl maleimide sensitive-factor attachment protein receptors (SNAREs). *Biophys J*. **87**, 3569-3584 (2004).
17. Liu, T., Tucker, W. C., Bhalla, A., Chapman, E. R., & Weisshaar, J. C. SNARE-driven, 25-millisecond vesicle fusion in vitro. *Biophys J*. **89**, 2458-2472 (2005).
18. Yoon, T. Y., Okumus, B., Zhang, F., Shin, Y. K., & Ha, T. Multiple intermediates in SNARE-induced membrane fusion. *Proc Natl Acad Sci U S A*. **103**, 19731-19736 (2006).
19. Diao, J. *et al.* A single-vesicle content mixing assay for SNARE-mediated membrane fusion. *Nat Commun*. **1**, 1-6 (2010).
20. Kyoung, M. *et al.* In vitro system capable of differentiating fast Ca2+-triggered content mixing from lipid exchange for mechanistic studies of neurotransmitter release. *Proc Natl Acad Sci U S A*. **108**, E304-313 (2011).
21. Domanska, M. K., Kiessling, V., Stein, A., Fasshauer, D., & Tamm, L. K. Single vesicle millisecond fusion kinetics reveals number of SNARE complexes optimal for fast SNARE-mediated membrane fusion. *J Biol Chem*. **284**, 32158-32166 (2009).
22. Kreutzberger, A. J., Kiessling, V., & Tamm, L. K. High Cholesterol Obviates a Prolonged Hemifusion Intermediate in Fast SNARE-Mediated Membrane Fusion. *Biophys J*. **109**, 319-329 (2015).
23. Schwenen, L. L. *et al.* Resolving single membrane fusion events on planar pore-spanning membranes. *Sci Rep*. **5**, 12006 (2015).
24. Karatekin, E. *et al.* A fast, single-vesicle fusion assay mimics physiological SNARE requirements. *Proc Natl Acad Sci U S A*. **107**, 3517-3521 (2010).
25. Karatekin, E., & Rothman, J. E. Fusion of single proteoliposomes with planar, cushioned bilayers in microfluidic flow cells. *Nat Protoc*. **7**, 903-920 (2012).
26. Smith, M. B. *et al.* Interactive, computer-assisted tracking of speckle trajectories in fluorescence microscopy: application to actin polymerization and membrane fusion. *Biophys J*. **101**, 1794-1804 (2011).
27. Stratton, B. S. *et al.* Cholesterol Increases the Openness of SNARE-Mediated Flickering Fusion Pores. *Biophys journal*. **110**, 1538–1550 (2016).

28. Diao, J. *et al.* Synaptic proteins promote calcium-triggered fast transition from point contact to full fusion. *Elife*. **1**, e00109 (2012).
29. Kiessling, V., Domanska, M. K., & Tamm, L. K. Single SNARE-mediated vesicle fusion observed in vitro by polarized TIRFM. *Biophys J*. **99**, 4047-4055 (2010).
30. Blasi, J. *et al.* Botulinum neurotoxin A selectively cleaves the synaptic protein SNAP-25. *Nature*. **365**, 160-163 (1993).
31. Washbourne, P. *et al.* Genetic ablation of the t-SNARE SNAP-25 distinguishes mechanisms of neuroexocytosis. *Nat Neurosci*. **5**, 19-26 (2002).
32. Diaz, A. J., Albertorio, F., Daniel, S., & Cremer, P. S. Double cushions preserve transmembrane protein mobility in supported bilayer systems. *Langmuir*. **24**, 6820-6826 (2008).
33. Floyd, D. L., Ragains, J. R., Skehel, J. J., Harrison, S. C., & van Oijen, A. M. Single-particle kinetics of influenza virus membrane fusion. *Proc Natl Acad Sci U S A*. **105**, 15382-15387 (2008).
34. Albertorio, F. *et al.* Fluid and air-stable lipopolymer membranes for biosensor applications. *Langmuir*. **21**, 7476-7482 (2005).
35. Daniel, S., Albertorio, F., & Cremer, P. S. Making lipid membranes rough, tough, and ready to hit the road. *Mrs Bulletin*. **31**, 536-540 (2006).
36. Gao, Y. *et al.* Single reconstituted neuronal SNARE complexes zipper in three distinct stages. *Science*. **337**, 1340-1343 (2012).
37. Kenworthy, A. K., Hristova, K., Needham, D., & Mcintosh, T. J. Range and Magnitude of the Steric Pressure between Bilayers Containing Phospholipids with Covalently Attached Poly(Ethylene Glycol). *Biophys J*. **68**, 1921-1936 (1995).
38. Knoll, W. *et al.* Solid supported lipid membranes: New concepts for the biomimetic functionalization of solid surfaces. *Biointerphases*. **3**, Fa125-Fa135 (2008).
39. Quinn, P., Griffiths, G., & Warren, G. Density of newly synthesized plasma membrane proteins in intracellular membranes II. Biochemical studies. *J Cell Biol*. **98**, 2142-2147 (1984).
40. Sund, S. E., Swanson, J. A., & Axelrod, D. Cell membrane orientation visualized by polarized total internal reflection fluorescence. *Biophys J*. **77**, 2266-2283 (1999).
41. Johnson, D. S., Toledo-Crow, R., Mattheyses, A. L., & Simon, S. M. Polarization-controlled TIRFM with focal drift and spatial field intensity correction. *Biophys J*. **106**, 1008-1019 (2014).
42. Anantharam, A., Onoa, B., Edwards, R. H., Holz, R. W., & Axelrod, D. Localized topological changes of the plasma membrane upon exocytosis visualized by polarized TIRFM. *J Cell Biol*. **188**, 415-428 (2010).
43. Axelrod, D. Carbocyanine dye orientation in red cell membrane studied by microscopic fluorescence polarization. *Biophys J*. **26**, 557-573 (1979).
44. Wang, T., Smith, E. A., Chapman, E. R., & Weisshaar, J. C. Lipid mixing and content release in single-vesicle, SNARE-driven fusion assay with 1-5 msec resolution. *Biophys J*. **96**, 4122-4131 (2009).
45. Chernomordik, L. V., Frolov, V. A., Leikina, E., Bronk, P., & Zimmerberg, J. The pathway of membrane fusion catalyzed by influenza hemagglutinin: restriction of lipids, hemifusion, and lipidic fusion pore formation. *J Cell Biol*. **140**, 1369-1382 (1998).
46. Takamori, S. *et al.* Molecular anatomy of a trafficking organelle. *Cell*. **127**, 831-846 (2006).
47. Wilhelm, B. G. *et al.* Composition of isolated synaptic boutons reveals the amounts of vesicle trafficking proteins. *Science*. **344**, 1023-1028 (2014).
48. Scott, B. L. *et al.* Liposome fusion assay to monitor intracellular membrane fusion machines. *Methods Enzymol*. **372**, 274-300 (2003).
49. Linkert, M. *et al.* Metadata matters: access to image data in the real world. *J Cell Biol*. **189**, 777-782 (2010).
50. Soumpasis, D. M. Theoretical analysis of fluorescence photobleaching recovery experiments. *Biophys J*. **41**, 95-97 (1983).
51. Ohki, S. A mechanism of divalent ion-induced phosphatidylserine membrane fusion. *Biochim Biophys Acta*. **689**, 1-11 (1982).
52. Berquand, A. *et al.* Two-step formation of streptavidin-supported lipid bilayers by PEG-triggered vesicle fusion. Fluorescence and atomic force microscopy characterization. *Langmuir*. **19**, 1700-1707 (2003).
53. Tamm, L. K., & McConnell, H. M. Supported phospholipid bilayers. *Biophys J*. **47**, 105-113 (1985).
54. Rawle, R. J., van Lengerich, B., Chung, M., Bendix, P. M., & Boxer, S. G. Vesicle fusion observed by content transfer across a tethered lipid bilayer. *Biophys J*. **101**, L37-39 (2011).
55. Wagner, M. L., & Tamm, L. K. Reconstituted syntaxin1a/SNAP25 interacts with negatively charged lipids as measured by lateral diffusion in planar supported bilayers. *Biophys J*. **81**, 266-275 (2001).
56. Kalb, E., Frey, S., & Tamm, L. K. Formation of Supported Planar Bilayers by Fusion of Vesicles to Supported Phospholipid Monolayers. *Biochimica Et Biophysica Acta*. **1103**, 307-316 (1992).

